A Sampling-Based Approach to Wideband Interference Cancellation

A. M. HAIMOVICH

M. O. BERIN

New Jersey Institute of Technology

J. G. TETI, JR.

Lambda Science, Inc.

Classical adaptive array schemes which use only complex spatial weights are inherently narrowband and consequently perform poorly when attempting to suppress wideband interference. The common solution to this problem is the use of tapped delay line filters in each spatial channel to facilitate space-time adaptive processing (STAP). The higher performance provided by the STAP architecture comes at the cost of a considerable increase in complexity. This paper presents a simpler technique based on programmable *time adjustable sampling* **(TAS) that provides a limited number of wideband degrees of freedom. Two TAS methods are introduced: TAS-sidelobe canceler (TAS-SLC) is based on the sidelobe canceler, while TAS-minimum variance beamformer (TAS-MVB) is derived from the minimum variance beamformer. TAS is implemented by adjusting the sampling instant at selected array channels. TAS-SLC consists of controlling the sampling in the main channel of the sidelobe canceler. With TAS-MVB array complex weights are substituted with TAS time delays. The performance of TAS methods with wideband interference is compared to the conventional sidelobe canceler and minimum variance beamformers. It is shown that TAS-SLC provides better performance than the sidelobe canceler, while TAS-MVB outperforms the minimum variance beamformer.**

Manuscript received October 6, 1994; revised August 22, 1996, January 3 and April 3, 1997.

IEEE Log No. T-AES/34/1/00173.

This work was supported in part by the Naval Air Warfare Center under Contract N62269-93-C-0536.

Authors' addresses: A. M. Haimovich and M. O. Berin, Electrical and Computer Engineering Department, Center for Communications and Signal Processing, New Jersey Institute of Technology, University Heights, Newark, NJ 07102; J. G. Teti, Jr., Lambda Science, Inc., P.O. Box 238, Wayne, PA 19087.

I. INTRODUCTION

Modern radar or communication systems use a variety of techniques to improve signal detection performance in environments with strong interference. Antenna related techniques take advantage of the spatial separation between the desired signal and interference to suppress the latter, provided the antenna has sufficiently low sidelobe characteristics. Adaptive algorithms, which are required to discriminate between interferences and useful signals, are often formulated as constrained optimization problems. Mainbeam (look direction) linear constraints that control the gain of the desired signal are commonly employed [1–3]. Two examples of mainbeam linear constraint beamforming algorithms are the *minimum variance beamformer* (MVB) [4–6], and the *linear prediction* (LP) *beamformer* [7]. The minimum variance (MV) method minimizes the output power of the array, subject to a mainbeam look direction preservation constraint. The LP beamformer estimates the interference present in the array beamformer output based on sampling the interference at individual channels or separate auxiliary channels, subject to the constraint that the main channel is not weighted. LP is a special case of the sidelobe canceler (SC) [8–11].

MV and LP when utilized with adaptive array schemes that support only complex spatial weights are inherently narrowband, and consequently perform poorly when attempting to suppress wideband interference. Wide bandwidth performance of adaptive arrays has been investigated by a number of researchers [5, 12–14]. In [12] it is shown that the increase in bandwidth results in a larger number of eigenvalues of the array correlation matrix crossing over the noise level eigenvalues. Each eigenvalue associated with the interference signal may be regarded as capturing a degree of freedom of the array. When additional degrees of freedom are not available, performance degradation ensues. The common solution to this problem is the use of tapped delay line filters in each array channel [15–17]. Tapped delay line filters add degrees of freedom that enable better control of the response of the array. Adaptive arrays that consist of both spatial and temporal weights are often referred to as space-time adaptive processing (STAP) arrays. A major difficulty of STAP processing schemes for many real-time applications is the availability of hardware that has the required computational speed and capacity.

Modern phased array radar and communication systems often have modular architectures, that utilize digital beamformers, with analog-to-digital (A/D) conversion at each spatial channel [18] (a specific implementation is given in [19]). After sampling in each channel, adaptive digital beamforming is performed by a real-time processing architecture.

In this work we study how *time adjustable sampling* (TAS) may be used to improve performance of adaptive arrays, particularly robustness to bandwidth effects. TAS is introduced through control of sampling instants in individual channels. TAS is suggested as a low-cast alternative to STAP, but also can be used with STAP if desired. Two TAS architectures are proposed and analyzed: TAS-SLC, derived from the sidelobe canceler LP/SC, and TAS-MVB, based on the MV beamformer. TAS-SLC requires information on the optimal time delay, however TAS-MVB does not require more information than conventional MVB. It is shown that TAS-MVB outperforms MV when the signal bandwidth is significant with respect to the carrier frequency. It is further shown that the SC performs poorly with wideband signals. TAS-SLC may be used to alleviate this problem.

Section II provides the problem formulation and definition of performance metrics. TAS is introduced and analyzed in Section III. Numerical results are presented in Section IV, and conclusions are contained in Section V.

II. PROBLEM FORMULATION

This section presents the signal model and introduces the efficiency as a performance metric. The situation considered here is that of a radar of relatively narrow bandwidth being irradiated by a wideband jammer. The jammer is considered wideband with respect to the radar carrier frequency. The effect of the bandwidth of the jammer is to decorrelate the signals received at the antenna array elements of the radar. The efficiency performance measure is normalized with respect to the target strength, hence the signal model refers only to the active interference. The efficiency of several conventional processing methods is computed in anticipation of the introduction of TAS.

A. Signal Model

The interference signal received at the nth element of an N-element array is the real part of the analytic signal

$$\tilde{r}_n(t) = r(t-\tau_n)e^{j\omega_c(t-\tau_n)} \tag{1}$$

where $r(t)$ is the complex envelope of the received signal, ω_c is the carrier angular frequency, and τ_n is the propagation delay across the array from the first to the nth element. After complex, coherent carrier demodulation, and filtering at the receiver, the signals are represented by their complex envelopes,

$$\begin{aligned} s_n(t) &= \int \tilde{r}_n(u)h(t-u)e^{-j\omega_c u}\,du \\ &= g(t-\tau_n)e^{-j\omega_c\tau_n} \end{aligned} \tag{2}$$

where the complex envelope $g(t) = \int r(u)h(t-u)\,du$ and $h(t)$ is the impulse response of the receiver. The process represented by the complex envelope $g(t)$ is considered *wideband* when variations in its autocorrelation function (ACF) across the array, $R_g(\tau_m-\tau_n) = E[g(t-\tau_n)g^*(t-\tau_m)]$, are nonnegligible. Consider an interference at an angle θ with respect to the array normal. If the interelement spacing is half-wavelength at the carrier frequency, then the received signal phase advance between two array elements is given by $\xi = \pi\sin\theta$. The propagation delay between the first and nth array elements measured at carrier frequency is then

$$\tau_n = (n-1)\frac{\xi}{\omega_c}. \tag{3}$$

The interference source produces an array vector

$$\mathbf{s}(t) = [s_1(t),\ldots,s_N(t)]^{\mathrm{T}} \tag{4}$$

where the superscript denotes transposition. The correlation matrix of the interference across the array is given by

$$\mathbf{R} = E[\mathbf{s}(t)\mathbf{s}(t)^{\mathrm{H}}] \tag{5}$$

where the superscript is the complex conjugate transpose. This correlation matrix consists of terms of the form:

$$\begin{aligned} \mathbf{R}(n,m) &= E[s_n(t)s_m^*(t)] \\ &= E[g(t-\tau_n)g^*(t-\tau_m)]e^{-j\omega_c(\tau_n-\tau_m)}. \end{aligned} \tag{6}$$

To be specific, let $R_g(\tau) = E[g(t)g^*(t-\tau)] = \sigma_I^2(1-\alpha|\tau|)$, for $|\tau| \le 1/\alpha$ and $R_g(\tau) = 0$ for $|\tau| > 1/\alpha$, where σ_I^2 is the power, and $\alpha \ge 0$ is a parameter that controls the decorrelation of the interference signal across the array. Larger values of α indicate wider bandwidth. Conversely, for $\alpha = 0$, the interference is a pure sinusoid. Using (3), the array correlation matrix for the interference source is then given by

$$\mathbf{R}(n,m) = \sigma_I^2\left(1-\frac{\alpha\xi}{\omega_c}|n-m|\right)e^{-j(n-m)\xi}. \tag{7}$$

For the narrowband case, $\alpha = 0$, and $\mathbf{R}$ can be expressed

$$\mathbf{R} = \sigma_I^2\mathbf{d}_I\mathbf{d}_I^{\mathrm{H}} \tag{8}$$

where $\mathbf{d}_I$ is the source *space vector* defined as

$$\mathbf{d}_I = \frac{1}{\sqrt{N}}[1,e^{-j\xi},\ldots,e^{-j(N-1)\xi}]^{\mathrm{T}}. \tag{9}$$

The space vector represents the phase progression of a received signal across the array. The array vector $\mathbf{z}(t)$ consists of the target and interference-plus-noise contributions

$$\begin{aligned} \mathbf{z}(t) &= \mathbf{m}(t) + \mathbf{x}(t) \\ &= \mathbf{m}(t) + \mathbf{s}(t) + \mathbf{v}(t) \end{aligned} \tag{10}$$

where $\mathbf{m}(t)$ represents the target return, and $\mathbf{v}(t)$ represents background white Gaussian noise with distribution $CN[\mathbf{0},\sigma_v^2\mathbf{I}]$. The notation CN is for the complex-valued Gaussian distribution, σ_v^2 is the noise power, and $\mathbf{I}$ is the N-dimensional identity matrix. The array interference-plus-noise correlation matrix is then given by

$$\mathbf{R}_x = \mathbf{R} + \sigma_v^2\mathbf{I}. \tag{11}$$

The array *efficiency* is a metric that quantifies the performance of the beamformer relative to the case when the interference is absent:

$$\eta = \frac{\mathrm{SINR}}{\mathrm{SNR}} \tag{12}$$

where SINR is the signal-to-interference plus noise ratio at the array output, and SNR is the signal-to-noise ratio at each array element when the interference is not present. Note that the efficiency depends only on the interference-to-noise ratio (INR) at the array output. Indeed,

$$\eta = \frac{\dfrac{S}{I_0+N}}{\dfrac{S}{N}} = \frac{N}{I_0+N} = \frac{1}{1+I_0/N} \tag{13}$$

where S, N, I_0, are respectively, the expected signal, noise, and interference power levels. The interference power in the previous expression is computed at the output of the array, and hence the efficiency in (12) characterizes the performance of the array for a specific interference scenario, i.e., interference angle variable ξ, and input INR, and is independent of the target power. Let $\mu = \sigma_I^2/\sigma_v^2$, denote the input INR. To assess global performance independent of INR, we define the *asymptotic efficiency* for INR $= \mu \to \infty$:

$$\eta_\infty = \lim_{\mu\to\infty} \eta. \tag{14}$$

Likewise, the performance averaged over all angles θ is represented by the *average efficiency*

$$\overline{\eta} = E_\theta[\eta] \tag{15}$$

where the notation E_θ represents expectation with respect to θ. Finally, when the averaging over the interference angle is done on the asymptotic efficiency, we obtain the *average asymptotic efficiency* (AAE)

$$\overline{\eta}_\infty = E_\theta[\eta_\infty]. \tag{16}$$

It will be shown in the sequel, that the AAE is a single figure that represents the performance of the array in terms of the number of elements and the interference time-bandwidth product (TBP).

Several beamformers are next introduced and their efficiency is evaluated. The discussion of the beamformers is necessarily concise. More details can be found in [6].

B. Quiescent Beamformer

In the absence of interference, the output SNR of the beamformer is maximized by the *quiescent* (unadapted) weight vector. Window functions (amplitude taper) are usually incorporated to lower the sidelobes. For simplicity, we assume no amplitude taper in our analysis. In radar array processing, for each antenna element, inphase and quadrature channel signals are processed by single pulse matched filters. Subsequently, the inphase and quadrature samples are combined to form a sample of the complex envelope, which is then weighted by a complex factor and summed with similarly processed quantities from the other antennas. This weighting and summing process is referred to as beamforming. The channel weights are usually represented in vector form. Let the target space vector be $\mathbf{d}_t$, obtained by substituting ξ in (9) with the appropriate quantity for the desired target. The quiescent weight vector that maximizes the output SNR in the absence of interferences is then just the matched filter to $\mathbf{d}_t$, and is given by [20] $\mathbf{w}_q = \mathbf{d}_t$. From the definition of the efficiency in (12), and the expression for the (unadapted) weight vector $\mathbf{w}_q = \mathbf{d}_t$, it follows that the efficiency

$$\eta = \frac{1}{\mu|\rho|^2 + 1} \tag{17}$$

where $\rho = \mathbf{d}_I^{\mathrm{H}}\mathbf{d}_t$. Without loss of generality, assume that the angle to the desired signal is $\theta_t = 0$. Then the inner product of the two space vectors $\mathbf{d}_I$ and $\mathbf{d}_t$ is given by $\rho = (1/N)\sum_{n=0}^{N-1} e^{jn\xi}$. Clearly, the unadapted beamformer has zero asymptotic efficiency, except when $\rho = 0$ (i.e., the interference happens to coincide exactly with a zero of the unadapted pattern).

C. Minimum Variance Beamformer

With the MV method, the array weight vector is designed to minimize the power at the output, subject to specified gain constraints [6]. The MV weight vector is given by

$$\mathbf{w}_{\mathrm{MV}} = c\mathbf{R}_x^{-1}\mathbf{d}_t \tag{18}$$

where c is a gain factor which does not affect the output SINR, and $\mathbf{d}_t$ represents the *direction of look*. It can be easily shown, that given the weights in (18), a target power of σ_t^2, and the correlation matrix (11) for a narrowband interference, we have

$$\begin{aligned}\mathrm{SINR} &= \sigma_t^2(\mathbf{d}_t^{\mathrm{H}}\mathbf{R}_x^{-1}\mathbf{d}_t)\\ &= \sigma_t^2\sigma_v^{-2}(1-\gamma|\rho|^2)\end{aligned} \tag{19}$$

where $\gamma = \mu/(1+\mu)$. Since SNR $= \sigma_t^2\sigma_v^{-2}$, the efficiency of the MV beamformer is given by

$$\eta = 1 - \gamma|\rho|^2. \tag{20}$$

The efficiency is conditioned on the interference angle through the variable ρ. This conditioning can be eliminated by regarding the angle as a random variable. Let the angle θ be uniformly distributed, and let $\xi = \pi \sin\theta$, then

$$E[e^{jn\xi}] = (1/2\pi)\int_{-\pi}^{\pi} e^{jn\pi\sin\theta}\,d\theta = \begin{cases} 1 & n = 0 \\ 0 & n \neq 0 \end{cases}. \tag{21}$$

It follows that $E[\mathbf{d}_I] = (1/\sqrt{N})\mathbf{u}_0$, where $\mathbf{u}_0^{\mathrm{T}} = [1,0,\ldots,0]$. It also follows that $E[\rho] = E[\mathbf{d}_I^{\mathrm{H}}\mathbf{d}_t] = 1/N$. The second moment is given by $E[|\rho|^2] = \mathbf{d}_t^{\mathrm{H}}E[\mathbf{d}_I\mathbf{d}_I^{\mathrm{H}}]\mathbf{d}_t = (1/N)\mathbf{d}_t^{\mathrm{H}}\mathbf{d}_t = 1/N$. The average efficiency, defined in (15), is obtained by substituting $E[|\rho|^2]$ for $|\rho|^2$ in (20),

$$\overline{\eta} = 1 - \frac{\gamma}{N} \tag{22}$$

where the symbol $\overline{\eta}$ is short notation for expectation of η. The AAE $\overline{\eta}_\infty$ can be computed noting that as $\mu \to \infty$, $\gamma \to 1$:

$$\overline{\eta}_\infty = \lim_{\gamma\to 1}\left(1 - \frac{\gamma}{N}\right) = 1 - \frac{1}{N}. \tag{23}$$

Note that in expressions (20), (22), and (23), the efficiency is always less than unity, i.e., the SINR in the presence of interference cannot be greater than the SNR when the interference is absent. The efficiency has another simple elegant interpretation: it is the average fractional number of degrees of freedom available *following* the cancellation of the interference. On average, an interference with infinite power captures a full degree of freedom ($1/N$ of the available), while when $\mu < \infty$, less than a degree of freedom is captured by the interference cancellation processing.

D. Sidelobe Canceler/Linear Predictor

We first introduce the LP beamformer, and then generalize it to the well known SC. With the LP method, the interference is predicted at a chosen array element (main channel) from samples taken at other elements (auxiliary channels). To the extent that those samples are correlated, the interference can be reduced by subtracting the predicted value from the signal in the main channel. This operation is equivalent to minimizing the array output power subject to the constraint that the weight vector component associated with the main channel is set to one [6]. The LP optimization problem thus reads,

$$\min_{\mathbf{w}} \mathbf{w}^{\mathrm{H}}\mathbf{R}_x\mathbf{w} \qquad \text{subject to} \quad \mathbf{w}^{\mathrm{H}}\mathbf{u}_0 = 1 \tag{24}$$

where $\mathbf{u}_0^{\mathrm{T}} = [1,0,\ldots,0]$. This formulation results in the weight vector:

$$\mathbf{w}_{\mathrm{LP}} = c\mathbf{R}_x^{-1}\mathbf{u}_0 \tag{25}$$

where, similar to the MV solution, c does not affect the output SINR. The SC may be viewed as an LP beamformer in which the gain of the main channel is larger than the gain of the auxiliary channels. Assume that the gain of the main channel is g. Then the space vector is given by

$$\tilde{\mathbf{d}}_I = \frac{1}{\sqrt{N}}[g, e^{-j\xi},\ldots,e^{-j(N-1)\xi}]^{\mathrm{T}} \tag{26}$$

where the ˜ symbol is used to distinguish this vector from the space vector $\mathbf{d}_I$. The modulus of the SC space vector is given by $h = \tilde{\mathbf{d}}_I^{\mathrm{H}}\tilde{\mathbf{d}}_I = (g + N - 1)/N$. The SC weight vector $\mathbf{w}_{\mathrm{SC}}$ is found by solving the optimization problem (24) with $\mathbf{R}_x$ replaced by $\tilde{\mathbf{R}}_x$, where the gain of the main channel is set to g. For example, for a single tone interference, (11) becomes $\tilde{\mathbf{R}}_x = \sigma_i^2\tilde{\mathbf{d}}_I\tilde{\mathbf{d}}_I^{\mathrm{H}} + \sigma_v^2\mathbf{I}$. Hence, the SC solution is given by (25), with $\mathbf{R}_x$ replaced by $\tilde{\mathbf{R}}_x$. We proceed with the computation of the efficiency of the SC. The efficiency of the LP method can be obtained by substituting $g = 1$ in the appropriate expressions. The weight vector for the narrowband, single source case is given by

$$\begin{aligned}\mathbf{w}_{\mathrm{SC}} &= \tilde{\mathbf{R}}_x^{-1}\mathbf{u}_0 \\ &= \sigma_v^{-2}(\mathbf{I} - \tilde{\gamma}\tilde{\mathbf{d}}_I\tilde{\mathbf{d}}_I^{\mathrm{H}})\mathbf{u}_0 \\ &= \sigma_v^{-2}\left(\mathbf{u}_0 - \tilde{\gamma}\frac{g}{\sqrt{N}}\tilde{\mathbf{d}}_I\right)\end{aligned} \tag{27}$$

where $\tilde{\gamma} \equiv \mu/(1 + \mu\tilde{\mathbf{d}}_I^{\mathrm{H}}\tilde{\mathbf{d}}_I)$, and $\tilde{\rho} \equiv \tilde{\mathbf{d}}_I^{\mathrm{H}}\tilde{\mathbf{d}}_t$. It follows that the SINR is given by

$$\begin{aligned}\mathrm{SINR} &= \sigma_t^2\frac{|\mathbf{w}_{\mathrm{SC}}^{\mathrm{H}}\tilde{\mathbf{d}}_t|^2}{\mathbf{w}_{\mathrm{SC}}^{\mathrm{H}}\tilde{\mathbf{R}}_x\mathbf{w}_{\mathrm{SC}}} \\ &= \sigma_t^2\frac{\sigma_v^{-4}\left|\left(\mathbf{u}_0 - \tilde{\gamma}\frac{g}{\sqrt{N}}\tilde{\mathbf{d}}_I\right)\tilde{\mathbf{d}}_t\right|^2}{\sigma_v^{-2}\mathbf{u}_0^{\mathrm{T}}(\mathbf{I} - \tilde{\gamma}\tilde{\mathbf{d}}_I\tilde{\mathbf{d}}_I^{\mathrm{H}})\mathbf{u}_0} \\ &= \sigma_t^2\sigma_v^{-2}\frac{\frac{g^2}{N}|1 - \tilde{\gamma}\tilde{\rho}|^2}{1 - \frac{g^2}{N}\tilde{\gamma}}.\end{aligned} \tag{28}$$

The efficiency of the SC conditioned on the interference angle and power is then given by

$$\eta = \frac{\frac{g^2}{N}|1 - \tilde{\gamma}\tilde{\rho}|^2}{1 - \frac{g^2}{N}\tilde{\gamma}}. \tag{29}$$

Note that due to the gain in the main channel, the efficiency could be larger than 1. For example, in the absence of interference $\tilde{\gamma} = 0$, hence $\eta = g^2/N$ which, depending on g, could be larger than 1. Regarding ρ as random variable, and setting the first channel gain to g, we get $E[\tilde{\rho}] = g^2/N$, and $E[|\tilde{\rho}|^2] =$

$(g^4 + N - 1)/N^2$. Using these moments in (28), yields the average efficiency

$$\overline{\eta} = \frac{\left[\left(1 - \tilde{\gamma}\frac{g^2}{N}\right)^2 + \tilde{\gamma}^2 \frac{N-1}{N^2}\right]}{1 - \tilde{\gamma}\frac{g^2}{N}}. \tag{30}$$

When the interference power is large, $\lim_{\mu\to\infty} \tilde{\gamma} = 1/\tilde{\mathbf{d}}_I^{\mathrm{H}}\tilde{\mathbf{d}}_I = N/(g^2 + N - 1)$. Substituting in the relation above, we obtain the AAE of the SC:

$$\overline{\eta}_\infty = \frac{g^2}{g^2 + N - 1}. \tag{31}$$

For a single narrowband interference source, to make the efficiency of the SC equal to that of the MV method in (23), set $g = (N-1)$. As previously mentioned, LP is obtained as a special case of the SC by setting $g = 1$. In this case the AAE is equal to

$$\overline{\eta}_\infty = \frac{1}{N}. \tag{32}$$

Both the MVB and LP exhibit performance degradation in the wideband interference case. Next, the efficiency is characterized for wideband signals.

E. Bandwidth Effects

When the interference bandwidth cannot be ignored, the array correlation matrix for each signal is given in the form of (6). The effect of bandwidth on the efficiency will be analyzed through the performance of the MV beamformer. From (19) and the definition of efficiency, we have for MV

$$\eta = \sigma_v^2 \mathbf{d}_t^{\mathrm{H}} \mathbf{R}_x^{-1} \mathbf{d}_t. \tag{33}$$

Let the spectral decomposition of the matrix $\mathbf{R}_x$ be $\mathbf{R}_x = \mathbf{Q}\mathbf{\Lambda}\mathbf{Q}^{\mathrm{H}}$, where the columns of $\mathbf{Q}$ are the eigenvectors of $\mathbf{R}_x$, and $\mathbf{\Lambda} = \mathrm{diag}(\lambda_1,\ldots,\lambda_N)$, where the λ's are the eigenvalues of $\mathbf{R}_x$. Let $\mathbf{b} = \mathbf{Q}^{\mathrm{H}}\mathbf{d}_t$, then the efficiency can be expressed $\eta = \sigma_v^2 \mathbf{b}^{\mathrm{H}}\mathbf{\Lambda}^{-1}\mathbf{b}$. In the narrowband case, the eigenvalues of $\mathbf{R}_x$ are $\lambda_1 = \sigma_I^2 + \sigma_v^2$, and $\lambda_2 = \cdots = \lambda_N = \sigma_v^2$. A wideband interference corresponds to several principal eigenvalues. Let r be the number of eigenvalues larger than σ_v^2. The argument leading to (20), can be recast in terms of the eigen-decomposition of $\mathbf{R}_x$ and generalized to the wideband case:

$$\begin{aligned}\eta &= \sigma_v^2 \mathbf{b}^{\mathrm{H}}\mathbf{\Lambda}^{-1}\mathbf{b}\\ &= 1 - \sum_{j=1}^{r}\left(1 - \frac{\sigma_v^2}{\lambda_j}\right)|b_j|^2\end{aligned} \tag{34}$$

where $b_j = \mathbf{q}_j^{\mathrm{H}}\mathbf{d}_t$, and $\mathbf{q}_j$ is the jth eigenvector of $\mathbf{R}_x$. The asymptotic efficiency is found by letting the r principal eigenvalues $\lambda_j \to \infty$:

$$\eta_\infty = 1 - \sum_{j=1}^{r}|b_j|^2. \tag{35}$$

The application of this expression to predict the efficiency in canceling wideband interference requires some consideration: given an interference with bandwidth B rad/s, what is r? The number of principal eigenvalues is predicted by the Landau–Pollak theorem [21]:

$$r = 2 \times \mathrm{TBP} + 1 \tag{36}$$

where TBP is given by $\mathrm{TBP} = B\tau_N/2\pi = (B/\omega_c)(0.5(N-1)\sin\theta)$. Even given r, the quantity $\sum_{j=1}^{r}|b_j|^2$ cannot be evaluated analytically, but since the orthonormal property of the eigenvectors requires $\sum_{j=1}^{N}|b_j|^2 = 1$, and if we assume that the target vector $\mathbf{d}_t$ has approximately equal projections over the eigenvectors, then $\sum_{j=1}^{r}|b_j|^2 \cong r/N$. In this case, the asymptotic efficiency can be expressed in terms of the bandwidth:

$$\begin{aligned}\eta_\infty &\cong 1 - \frac{r}{N}\\ &\cong 1 - \frac{(B/\omega_c)(N-1)\sin\theta + 1}{N}.\end{aligned} \tag{37}$$

This expression indicates that the efficiency degrades proportionally with the rank of the interference subspace. Since the rank is proportional to the interference bandwidth, it follows that an increase in bandwidth has the effect of capturing an increasing number of degrees of freedom.

In view of the fact that a wider bandwidth requires more degrees of freedom, one way to compensate for bandwidth effects is to increase the number of degrees of freedom. This is precisely what is achieved by applying STAP.

F. STAP

STAP consists of an antenna array and a tap-delay line at each antenna. Let the number of taps be M and the delay at each tap be q seconds. It follows that the phase advance between taps is $\omega_c q$. We form the source array matrix

$$\mathbf{S}(t) = \begin{bmatrix} s(t) & \cdots & s(t-\tau_{1,M})\\ \vdots & & \vdots\\ s(t-\tau_{N,1}) & \cdots & s(t-\tau_{N,M})\end{bmatrix} \tag{38}$$

where $\tau_{n,m}$ is the time propagation delay between the first antenna element and the mth tap delay at the nth antenna, and is given by (see Fig. 1):

$$\begin{aligned}\tau_{n,m} &= \frac{\Delta\phi_{n,m}}{\omega_c}\\ &= (n-1)\xi/\omega_c + (m-1)q\end{aligned} \tag{39}$$

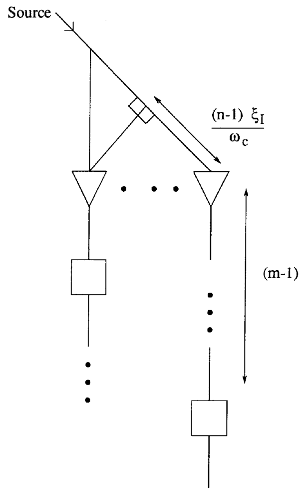

Fig. 1. Computation of time delay in STAP.

for $1 \le n \le N$, $1 \le m \le M$ and where $\phi_{n,m}$ is the phase associated with $\tau_{n,m}$. We now form the space-time array vector by stacking the elements of $\mathbf{S}(t)$ in a column-wise fashion. The resulting source vector for the space-time array is given by

$$\mathbf{s}(t) = \mathbf{H}(t)\,\mathbf{d}_I \tag{40}$$

where $\mathbf{H}(t)$ is the $NM \times NM$ matrix

$$\mathbf{H}(t) = \mathrm{diag}[g(t),\ldots,g(t-\tau_{N,M})] \tag{41}$$

and $\mathbf{d}_I$ is the NM-dimensional space-time vector

$$\mathbf{d}_I = \frac{1}{\sqrt{NM}}[1, e^{-j\xi},\ldots,e^{-j((N-1)\xi+(M-1)\omega_c q)}]^{\mathrm{T}}. \tag{42}$$

The space-time covariance matrix is given by $\mathbf{R} = E[\mathbf{s}(t)\mathbf{s}^{\mathrm{H}}(t)]$. Given the ACF $R_g(\tau) = \sigma_I^2(1-\alpha|\tau|)$, the space-time covariance matrix has terms $\mathbf{R}(\tau_{n,m}-\tau_{l,k})$, $1 \le m$, $k \le M$, $1 \le n$, $l \le N$. We have

$$\begin{aligned}\mathbf{R}(\tau_{n,m}-\tau_{l,k}) &= \sigma_I^2(1-\alpha|\tau_{n,m}-\tau_{l,k}|)e^{-j\omega_c(\tau_{n,m}-\tau_{l,k})}\\ &= \sigma_I^2(1-\alpha|(n-l)\xi/\omega_c-(m-k)q|)\\ &\quad\times e^{-j((n-l)\xi-(m-k)\omega_c q)}.\end{aligned} \tag{43}$$

For a single narrowband source ($\alpha \approx 0$), the space-time covariance matrix has the same form as (11), except $\mathbf{d}_I$ is now the vector defined in (42). The AAE of the space-time MV beamformer is found following computations similar to those for the MV beamformer, and is given by

$$\overline{\eta}_\infty = 1 - \frac{1}{NM}. \tag{44}$$

When the source is wideband, the efficiency is analogous to expression (33)

$$\eta = \sigma_v^2\mathbf{d}_t^{\mathrm{H}}\mathbf{R}_x^{-1}\mathbf{d}_t \tag{45}$$

where $\mathbf{d}_t$ represents the space-time direction of look.

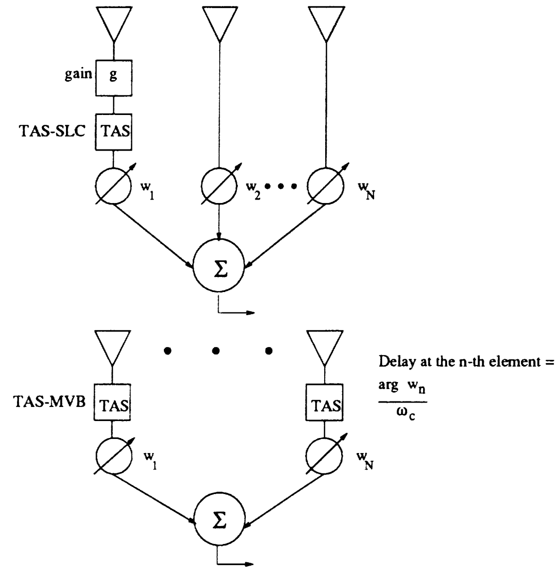

Fig. 2. TAS-SLC and TAS-MVB array configurations.

III. TIME ADJUSTABLE SAMPLING METHOD

Two TAS methods are formulated: TAS-SLC is derived from the side-lobe canceler, and TAS-MVB is based on the MV beamformer. With TAS-SLC, the main channel is sampled with a delay/advance relative to the other channels. For brevity, we consider only *delays*, since a time advance is just a negative time delay. TAS-MVB consists of implementing the MV weights using *time delays* rather than *phase shifts*. The time delays are implemented by adjusting the sampling instants. In a conventional digital beamformer all channels are sampled simultaneously. The TAS idea is to control the sampling instant of the individual channels. This provides additional degrees of freedom for processing which, as shown in the sequel, can improve performance with respect to wideband interference cancellation. TAS can be implemented by direct control of the A/D device in each channel. The two TAS configurations are shown schematically in Fig. 2. In both cases, the sampling takes place following coherent carrier demodulation and single pulse matched filtering, hence it affects only the complex envelope of the received signal. TAS is only intended to compensate for the decorrelation of the interference across the antenna array. Therefore, the time delays involved are of the same magnitude scale as the propagation delays across the array. These delays are typically much smaller than those required to cause a significant change in the range-Doppler ambiguity function and therefore, should not affect the range response. A typical example is provided at the end of Section IV.

For both methods, TAS-SLC and TAS-MVB, we assume that the array covariance matrix is computed *prior* to the sampling time adjustments. Appropriate time delays are then computed and applied. It is shown that the effect of the time delays is equivalent to the application of frequency dependent weights. We now proceed to formulate the two TAS methods.

TAS-SLC consists of adding a time delay δ_1 in the main channel of the SC. The TAS-SLC output can be written $y(t) = w^{\mathrm{H}}\mathbf{z}_{\delta_1}(t)$, where $\mathbf{z}_{\delta_1}(t) = \mathbf{m}_{\delta_1}(t) + \mathbf{x}_{\delta_1}(t)$, $\mathbf{m}_{\delta_1}(t)$, $\mathbf{x}_{\delta_1}(t)$ are defined as in (10) except for the delay in the main channel, i.e., $\mathbf{x}_{\delta_1}(t) = [x_1(t-\delta_1), x_2(t), \ldots, x_N(t)]$, and $\mathbf{w}$ is the weight vector. The contribution of the first channel only to the output can be written $w_1^* x_1(t-\delta_1)$, where w_1^* is the complex conjugate of the weight applied to the main channel. The time delay has the effect of a frequency-dependent complex weight. This can be seen from the frequency domain representation of $w_1^* x_1(t-\delta_1)$:

$$\begin{aligned}\mathcal{F}[w_1^* x_1(t-\delta_1)] &= \int_{-\infty}^{\infty} w_1^* x_1(t-\delta_1) e^{-j\omega t}\, dt \\ &= (w_1 e^{j\omega\delta_1})^* X_1(\omega) \qquad (46)\end{aligned}$$

where $X_1(\omega)$ is the Fourier transform of $x_1(t)$ and $(w_1 e^{j\omega\delta_1})$ is the frequency-dependent complex weight. To find an expression for the TAS-SLC weights, denote the interference-plus-noise covariance matrix $\tilde{\mathbf{R}}_x(\delta_1) = E[\mathbf{x}_{\delta_1}(t)\mathbf{x}_{\delta_1}^{\mathrm{H}}(t)]$. Then in analogy with (27), we have

$$\mathbf{w}_{\mathrm{TS}} = \tilde{\mathbf{R}}_x^{-1}(\delta_1)\mathbf{u}_0. \qquad (47)$$

TAS-SLC performance is analyzed in the next section.

The TAS-MVB weight vector is implemented by adjusting the sampling instant in each channel such that it results in a phase shift at carrier frequency equal to the phase shift of the corresponding MV complex weight. Let w_n be the nth element of the MV weight vector. Then w_n can be written $w_n = |w_n| e^{j\arg w_n}$. The nth time delay is then given by

$$\delta_n = \frac{\arg w_n}{\omega_c}. \qquad (48)$$

This relation holds only if $\arg w_n$ is "unwrapped," i.e., as the index n is increased, the phase is advanced by $\pm 2\pi$ each time it changes sign. While the frequency-dependent phase shift is provided by the sampling delay, it is still necessary to apply the weight gain $|w_n^*|$. The result is $|w_n^*| x_n(t-\delta_n)$. In the frequency domain, $|w_n^*| e^{-j\omega\delta_n} X_n(\omega) = (w_n e^{j›\,\delta_n})^* X_n(\omega_c + ›\,)$, where › is the frequency shift from the carrier frequency. Thus the effect of the time delay is equivalent to a complex weight having a phase which is linearly varying with the size of the offset from the carrier frequency. The nth element of the TAS-MVB weight vector can then be written

$$\begin{aligned}w_{\mathrm{TM},n}(›\,) &= |w_n| e^{j\arg w_n} e^{j›\,\delta_n} \\ &= w_n e^{j›\,\delta_n}. \qquad (49)\end{aligned}$$

The efficiency of TAS methods can be computed from the definition in (12). Without loss of generality, assume that the desired target is at broadside, i.e., $\mathbf{d}_t = (1/\sqrt{N})[1,\ldots,1]^{\mathrm{T}}$. In the following relations, the weight vector $\mathbf{w}$ is to be substituted with either the SC or the MV weight vectors, expressions (27) and (18), respectively (note that $\mathbf{w}$ has nothing to do with the frequency-dependent gain in (49)). The following notation is introduced: let $\boldsymbol{\Delta} = [\delta_1,\ldots,\delta_N]^{\mathrm{T}}$ be the vector of time delays, then $\mathbf{m}_{\boldsymbol{\Delta}}(t) = [m_1(t-\delta_1),\ldots,m_N(t-\delta_N)]^{\mathrm{T}}$ is the target vector with delays, $\mathbf{R}_m(\boldsymbol{\Delta}) = (\sigma_t^2/\sigma_v^2)^{-1} E[\mathbf{m}_{\boldsymbol{\Delta}}(t)\mathbf{m}_{\boldsymbol{\Delta}}^{\mathrm{H}}(t)]$ is the target (normalized) correlation matrix. Similarly, let $\mathbf{x}_{\boldsymbol{\Delta}}(t) = [x_1(t-\delta_1),\ldots,x_N(t-\delta_N)]^{\mathrm{T}}$ be the interference-plus-noise vector with delays, and let $\mathbf{R}_x(\boldsymbol{\Delta}) = E[\mathbf{x}_{\boldsymbol{\Delta}}(t)\mathbf{x}_{\boldsymbol{\Delta}}^{\mathrm{H}}(t)]$ be the interference-plus-noise correlation matrix, when TAS is applied. Note that with TAS-SLC, $\boldsymbol{\Delta}$ has only a single non-zero component. According to definition (12), the efficiency is the ratio of SINR to SNR. We have

$$\mathrm{SINR} = \frac{\mathbf{w}^{\mathrm{H}} E[\mathbf{m}_{\boldsymbol{\Delta}}(t)\mathbf{m}_{\boldsymbol{\Delta}}^{\mathrm{H}}(t)]\mathbf{w}}{\mathbf{w}^{\mathrm{H}} E[\mathbf{x}_{\boldsymbol{\Delta}}(t)\mathbf{x}_{\boldsymbol{\Delta}}^{\mathrm{H}}(t)]\mathbf{w}}. \qquad (50)$$

Accounting for the preceding definitions of $\mathbf{R}_m(\boldsymbol{\Delta})$ and $\mathbf{R}_x(\boldsymbol{\Delta})$, it follows that the TAS array efficiency is given by

$$\eta = \frac{\mathbf{w}^{\mathrm{H}}\mathbf{R}_m(\boldsymbol{\Delta})\mathbf{w}}{\mathbf{w}^{\mathrm{H}}\mathbf{R}_x(\boldsymbol{\Delta})\mathbf{w}}. \qquad (51)$$

This expression is used to provide numerical evaluations of the efficiency of TAS in the next section.

IV. PERFORMANCE EVALUATION

In this section, conventional beamformers (MV\LP\SC) are compared with their TAS variants. All curves shown in the figures are numerical evaluations of the appropriate expressions. The bandwidth parameter "beta" appearing in the legends of some of the figures mentioned below, is defined from (7), as $\beta/(N-1)\pi = \alpha/\omega_c$. The physical interpretation of $(1-\beta)$ is the normalized magnitude of the correlation between the first and last elements of the array when the source is at $\theta = 90$ deg with respect to the array normal. Indeed, from (7),

$$\left.\frac{|\mathbf{R}(1,N)|}{\mathbf{R}(1,1)}\right|_{\theta=90} = 1-\beta. \qquad (52)$$

For example, the meaning of $\beta = 1$, is that signal received at the first and last array elements from an interference source at $\theta = 90$ deg are not correlated. Thus β controls the interference bandwidth.

The dependence of the efficiency on the time delay in TAS-SLC is shown in Fig. 3 for a scenario with parameters as follows: number of antenna elements $N = 8$, interference angle $\theta = 20$ deg, $\beta = 0.6$, input INR = 10 dB, SC main channel gain $g = (N-1) = (8-1) = 7$. The delay on the abscissa is normalized to $N\xi$ where $\xi = \pi \sin\theta$. The efficiency was computed

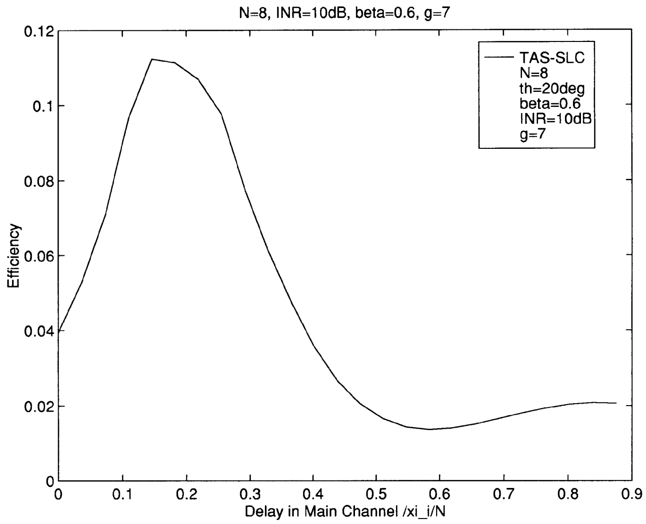

Fig. 3. TAS-SLC efficiency as function of time delay in main channel.

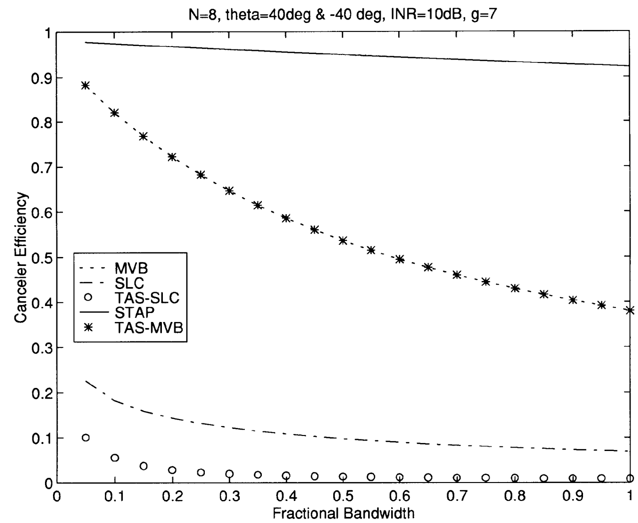

Fig. 5. Efficiency as function of bandwidth for two interference sources.

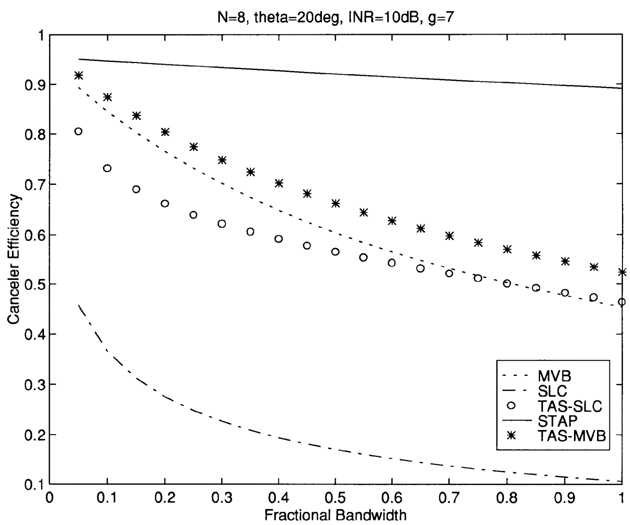

Fig. 4. Efficiency as function of bandwidth for one interference source.

numerically using (51) with the weight vector given by (47). Notice that at a normalized delay of 0.15, TAS provides a four times improvement in efficiency over SC (the efficiency of SC is found at zero time delay). A normalized time delay of 0.15 is used for TAS-SLC in the subsequent evaluations. The efficiency as a function of the normalized bandwidth β, is shown in the next several figures for different illustrative scenarios. The efficiency in each case was computed using (51). For the SC, $\boldsymbol{\Delta} = \mathbf{0}$, and the weight vector is given by (27); for TAS-SLC, the same weight vector (magnitude only in the main channel) is used with the appropriate delay in the main channel; for MV the weight vector is given by (18), and $\boldsymbol{\Delta} = \mathbf{0}$; for TAS-MVB, the magnitude of the weight vector in (18) is used with the delays in (48). STAP with $M = 2$ taps is included for comparison. The STAP efficiency was computed using (45).

Fig. 4 shows the efficiency versus the bandwidth parameter β for the case of one source at 20 deg. The efficiency of SLC is clearly very sensitive to the bandwidth and much inferior to all other methods. TAS-SLC makes SLC perform almost as well as MVB. The efficiency of the MV is reduced to 0.5 when the bandwidth reaches $\beta = 1$. TAS-MVB provides higher efficiency than MVB alone, but below that of STAP. An interesting case is shown in Fig. 5. The scenario consists of two interferences located symmetrically with respect to broadside at ± 40 deg. This is a worst case of sorts for both TAS-SLC and TAS-MVB, since a delay helping one source is also working against the other. The two sources require opposite signs which cannot be satisfied simultaneously, TAS should not result in any improvement. This is indeed evident in Fig. 5. Both SC and TAS-SLC perform poorly with multiple interferences. Fig. 6 represents the case of three equal power interferences located on the same side of broadside at 30, 40, and 50 deg, respectively. Again, TAS-MVB outperforms MV, but STAP does better than both. SC and TAS-SLC provide poor performance in the last two cases. The performance as a function of INR for a single interference source at 20 deg and bandwidth $\beta = 0.6$ is investigated in Fig. 7. As the INR increases, more degrees of freedom are captured, and the efficiency is reduced. STAP consistently provides the best performance, and TAS-SLC, TAS-MVB outperform MV for INR < 10 dB. Finally, Fig. 8 shows the efficiency as a function of the interference angle for each of the methods. The arrays are adapted with a single interference whose angle is varied. The efficiency of all methods goes to zero as the interference sweeps over the target (0 deg). It is interesting to note that TAS-MVB consistently outperforms MV. TAS-SLC provides consistently better performance than the SC

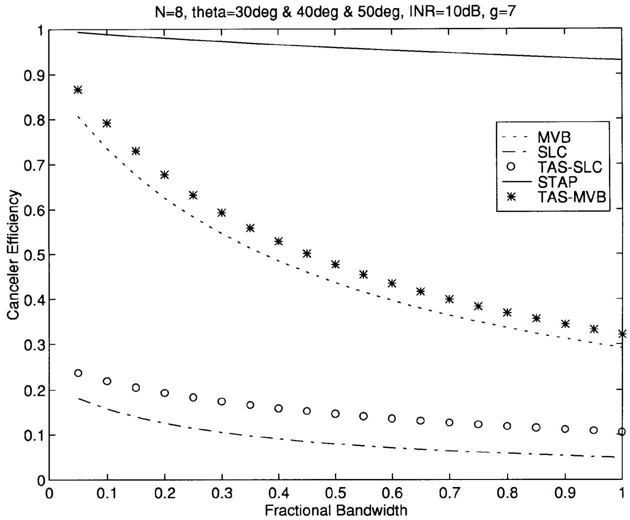

Fig. 6. Efficiency as function of bandwidth for three interference sources.

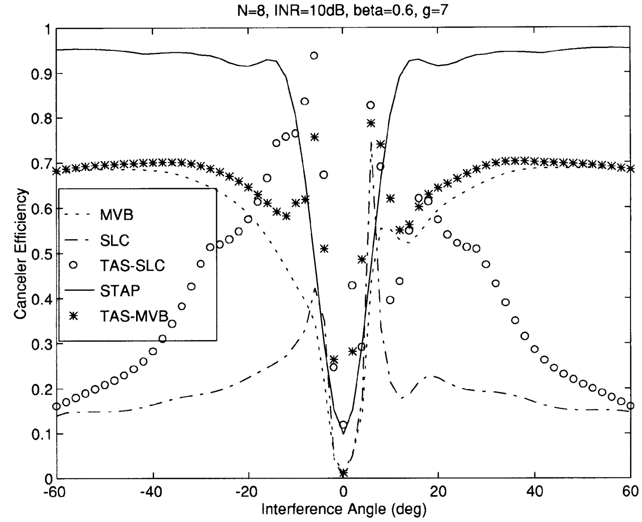

Fig. 8. Efficiency as function of interference angle.

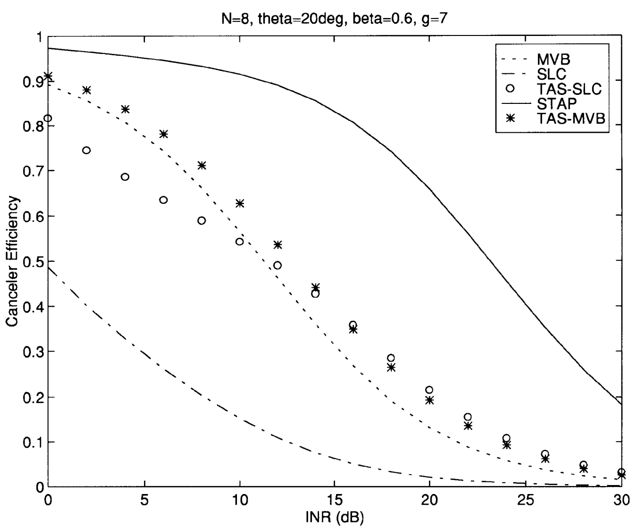

Fig. 7. Efficiency as function of INR for single interference.

and its performance is on par with MVB in a narrow angular region.

An issue worth noting is the size and resolution of the time delays required for TAS implementation. In the examples cited above, a normalized delay of 0.15, i.e., $0.15\xi N$, was required. Small delays are the ones difficult to implement, so let $\xi \approx 0.3\pi$ corresponding to an interference angle of 17 deg. At 500 MHz, $0.15\xi N \approx 0.3$ ns. From Fig. 3 it can be seen that an accuracy required is about $\pm 0.05\xi N = 0.1$ ns.

V. CONCLUSIONS

This paper presents a simple method for improving the performance of adaptive arrays with wideband interference. The method has been demonstrated for use with the SC or the MVB. It consists of adjusting the sampling instants of the array channels to achieve specified time delay/advance. The array efficiency is defined as a metric and is used to compare the performance of TAS methods with conventional beamformers. It is shown that for a single interference TAS-SLC provides a higher efficiency than the SC, however it requires information on the optimal time delay. Both the SC and TAS-SLC perform poorly when there are multiple interference sources. TAS-MVB is shown to consistently outperform the conventional MVB across a range of values for the bandwidth, INR or interference angle, and for single or multiple interferences. TAS-MVB is quite simple to implement, it does not require more information than conventional MVB, and can be used as a cost efficient enhancement to the MVB.

REFERENCES

[1] Applebaum, S. P., and Chapman, D. J. (1976)
Adaptive arrays with main beam constraints.
IEEE Transactions on Antennas Propagation, **24** (Sept. 1976), 650–662.

[2] Frost, O. L., III (1972)
An algorithm for linearly constrained adaptive array processing.
Proceedings of the IEEE, **60** (Aug. 1972), 926–935.

[3] Takao, K., Fujita, M., and Nishi, T. (1976)
An adaptive antenna array under directional constraint.
IEEE Transactions on Antennas Propagation, **24** (Sept. 1976), 662–669.

[4] Buckley, K. M. (1987)
Spatial/spectral filtering with linearly constrained minimum variance beamformers.
IEEE Transactions on Acoustics, Speech, and Signal Processing, **ASSP-35** (Mar. 1987), 249–266.

[5] Compton, R. T., Jr. (1988)
Adaptive Antennas.
Englewood Cliffs, NJ: Prentice Hall, 1988.

[6] Johnson, D. H., and Dudgeon, D. E. (1993)
Array Signal Processing: Concepts and Techniques.
Englewood Cliffs, NJ: Prentice Hall, 1993.

[7] Johnson, D. H. (1982)
The application of spectral estimation methods to bearing estimation problems.
Proceedings on the IEEE, **70** (Sept. 1982), 1018–1028.

[8] Skolnik, M. I. (1990)
Radar Handbook (2nd ed.).
New York: McGraw-Hill, 1990.

[9] Gabriel, W. F. (1980)
Spectral analysis and adaptive array superresolution techniques.
Proceedings of the IEEE, **68** (June 1980), 654–666.

[10] Hung, E. K. L. (1985)
Adaptive sidelobe cancellation by linear prediction.
In *Proceedings of the IEEE 1985 International Radar Conference*, 1985, 286–291.

[11] Yuen, S. M. (1989)
Algorithmic, architectural, and beam pattern issues of sidelobe cancellation.
IEEE Transactions on Aerospace and Electronic Systems, **25** (July 1989), 459–472.

[12] Mayhan, J. T. (1979)
Some techniques for evaluating the bandwidth characteristics of adaptive nulling systems.
IEEE Transactions on Antennas Propagation, **AP-27**, 3 (May 1979).

[13] Monzingo, R., and Miller, T. (1980)
An Introduction to Adaptive Arrays.
New York: Wiley, 1980.

[14] Hudson, J. E. (1981)
Adaptive Array Principles.
London: Peter Peregrinus, 1981.

[15] Rodgers, W. E., and Compton, R. T., Jr. (1979)
Adaptive array bandwidth with tapped delay-line processing.
IEEE Transactions on Aerospace and Electronic Systems, **AES-15**, 1 (Jan. 1979).

[16] Mayhan, J. T., Simmons, A. J., and Cummings, W. C. (1979)
Wideband adaptive antenna nulling using tapped delay lines.
Technical report 1979-45, M.I.T. Lincoln Laboratory, Lexington, MA, June 1979 (prepared under Contract F19628-78-C0002 for the Department of the Air Force and the Defense Communications Agency).

[17] Farina, A. (1992)
Antenna-Based Signal Processing Techniques for Radar Systems.
Dedham, MA: Artech House, 1992.

[18] Steyskal, H. (1987)
Digital beamforming antennas—An introduction.
Microwave Journal (Jan. 1987), 107–124.

[19] Teti, J. G., Jr., Jemison, W. D., Kim, S. H., Laska, J. E., Jr., and Halpern, H. M. (1993)
Wideband airborne early warning (AEW) radar.
In *Proceedings of the IEEE 1993 National Radar Conference*, Boston, Apr. 1993.

[20] Scharf, L. L. (1991)
Statistical Signal Processing Detection, Estimation and Time Series Analysis.
Reading, MA: Addison-Wesley, 1991.

[21] Slepian, D., and Pollak, H. O. (1962)
Prolate spheroidal wave functions Fourier analysis and uncertainty—III: The dimension of the space of essentially time- and band-limited signals.
The Bell System Technical Journal (July 1962), 1295–1336.

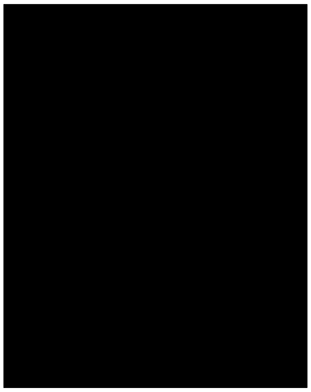

Alexander Haimovich received the B.S. degree from the Technion Institute of Technology, Israel, the M.S. degree from Drexel University, Philadelphia, PA, both in electrical engineering, and the Ph.D. degree in systems from the University of Pennsylvania, Philadelphia, in 1977, 1982, and 1989, respectively.

He is currently an Associate Professor of Electrical Engineering at the New Jersey Institute of Technology. His professional record includes positions at JJM Systems, Ivyland, PA as Chief Scientist from 1990 to 1992, and at American Electronic Laboratories, Lansdale, PA as Senior Staff Consultant from 1989 to 1990. Prior to this Dr. Haimovich was a Lecturer at the New Jersey Institute of Technology from 1987 to 1989 and a Senior Engineer at American Electronic Laboratories from 1983 to 1987. His research interests include adaptive arrays with applications to radar and mobile communications signal processing and signal separation in multiuser communication systems.

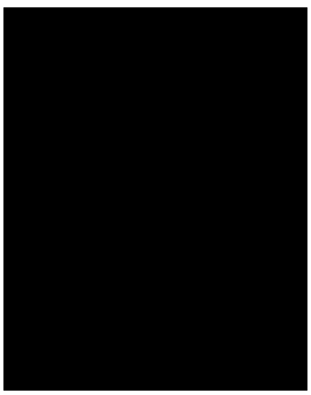

Murat O. Berin was born in Istanbul, Turkey, on May 22, 1970. He received the B.S. and M.S. degrees in 1994 and 1996 from the New Jersey Institute of Technology (NJIT), in electrical engineering.

From 1994 to 1996, he was a research assistant in Center for Communications and Signal Processing Research, NJIT, involved in a joint project with the U.S. Air Force. He is currently employed by Expert Wireless Solutions Inc., Fort Lee, NJ.

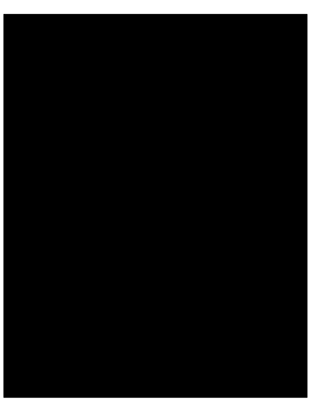

Joseph G. Teti, Jr. (S'90—M'91) received the B.S. degree from Drexel University, Philadelphia, PA in 1985, and the M.S.E. and Ph.D. degrees from the University of Pennsylvania in 1989 and 1991, respectively, all in electrical engineering.

He was a staff engineer with Flam and Russell, Inc., Horsham, PA from 1985 to 1987. From 1987 to 1992 he was with the Naval Air Development Center (NADC), Warminster, PA. From 1989 to 1991 he was on leave as an NADC Ph.D. Fellow at the Moore School of Electrical Engineering, University of Pennsylvania. In 1992 he returned to industry, he founded Lambda Science, Inc., Wayne, PA in 1995 where he is currently the Chief Scientist.

Dr. Teti's research interests are very broad and span topic areas that pertain to the design and application of advanced sensors. He has experience in advanced radar sensor system design and applications that include instrumentation, surveillance, tactical, surface search and synthetic aperture radar. His experience includes RF hardware covering areas from devices to antennas, theoretical and applied advanced signal processing techniques that emphasize the extraction and utilization of available sensor information, and the analysis of propagation and scattering phenomenology for the purposes of mitigation and/or exploitation.

Dr. Teti is a member of SIAM, The Association of Old Crows, Tau Beta Pi and Sigma Xi.